Available online at www.sciencedirect.com
SCIENCE DIRECT®
ELSEVIER
Journal of Chromatography A, 982 (2002) 85–95
JOURNAL OF CHROMATOGRAPHY A
www.elsevier.com/locate/chroma

Mapping of protein:protein contact surfaces by hydrogen/deuterium exchange, followed by on-line high-performance liquid chromatography–electrospray ionization fourier-transform ion-cyclotron-resonance mass analysis ☆

TuKiet T. Lam[a], Jason K. Lanman[b], Mark R. Emmett[a,c], Christopher L. Hendrickson[a,c], Alan G. Marshall[a,c,*], Peter E. Prevelige[b]

[a]*Department of Chemistry and Biochemistry, Florida State University, Tallahassee, FL 32306, USA*
[b]*Department of Microbiology, University of Alabama, Birmingham, AL 35294, USA*
[c]*National High Magnetic Field Laboratory, Florida State University, 1800 East Paul Dirac Drive, Tallahassee, FL 32310, USA*

Received 23 March 2002; received in revised form 14 August 2002; accepted 23 August 2002

Abstract

For protein complexes too large, uncrystallizable/insoluble, or low concentration for conventional X-ray diffraction or nuclear magnetic resonance analysis, the contact surface(s) may be mapped by comparing $H/^2H$ exchange rate (and thus solvent accessibility) of backbone amide hydrogens in free vs. complexed protein(s). The protein is first exposed to ^2H_2O, allowed to exchange for each of several reaction periods, and then digested with pepsin. The extent and rate of $H/^2H$ exchange is determined by measuring the increase in mass with $H/^2H$ exchange period for each of the peptides. Here, we present an experimental protocol that combines rapid (to minimize back-exchange) HPLC front-end separation with ultrahigh-resolution mass analysis (needed to distinguish the isotopic distributions of dozens of peptides simultaneously). The method is used to study the assembled human immunodeficiency virus type capsid protein (CA) and its soluble form.

Keywords: Viruses; Human immunodeficiency virus; Capsid; Ion cyclotron resonance; Mass spectrometry; Hydrogen–deuterium exchange; Proteins

1. Introduction

The methods of choice for determination of the three-dimensional structures of proteins and their complexes at atomic resolution are X-ray crystal diffraction [1–4] and high-resolution solution-phase nuclear magnetic resonance (NMR) [5–9]. However, both methods require large (typically multi-milligram) amounts of protein, and the protein must either be crystallizable to high diffraction order (X-ray) or relatively low molecular mass and soluble (NMR). With the increasing interest in protein assemblies, these requirements are not always realizable, and one is led to seek other approaches.

☆Presented at the 21st International Symposium on the Separation of Proteins, Peptides and Polynucleotides, Orlando, FL, 11–14 November, 2001.

*Corresponding author.

0021-9673/02/$ – see front matter
PII: S0021-9673(02)01357-2

It is particularly informative to identify the solvent-accessible surfaces of a protein, revealed by solution-phase hydrogen/deuterium ($H/^2H$) exchange, an approach for which the number of publications has doubled over the past decade [10]. $H/^2H$ exchange [11–15] is especially powerful when combined with high-resolution NMR [16–20], because one can simultaneously monitor $H/^2H$ exchange at each assigned amide hydrogen resonance, in an experiment tuned to detect only those protons directly bonded to nitrogen. However, such experiments are still limited by the usual NMR constraints of solubility and small protein size.

More recently, the $H/^2H$ exchange approach has been adapted to mass spectrometry [21–23]. The basic instrumental set-up is shown in Fig. 1. A dilute protein in H_2O solution is suddenly diluted with ^2H_2O buffer. The exchangeable hydrogens (namely the backbone amide hydrogens and various side-chain hydrogens) are then replaced by deuteriums over time. The rate of uptake of deuterium is experimentally determined by quenching the exchange (by reducing the pH and freezing the sample), cleaving the protein with pepsin, and then measuring the increase in mass of each of the peptic peptides by liquid chromatography–mass spectrometry (LC–MS). Advantages of this approach are that only a small amount (typically 1 μg per sample)

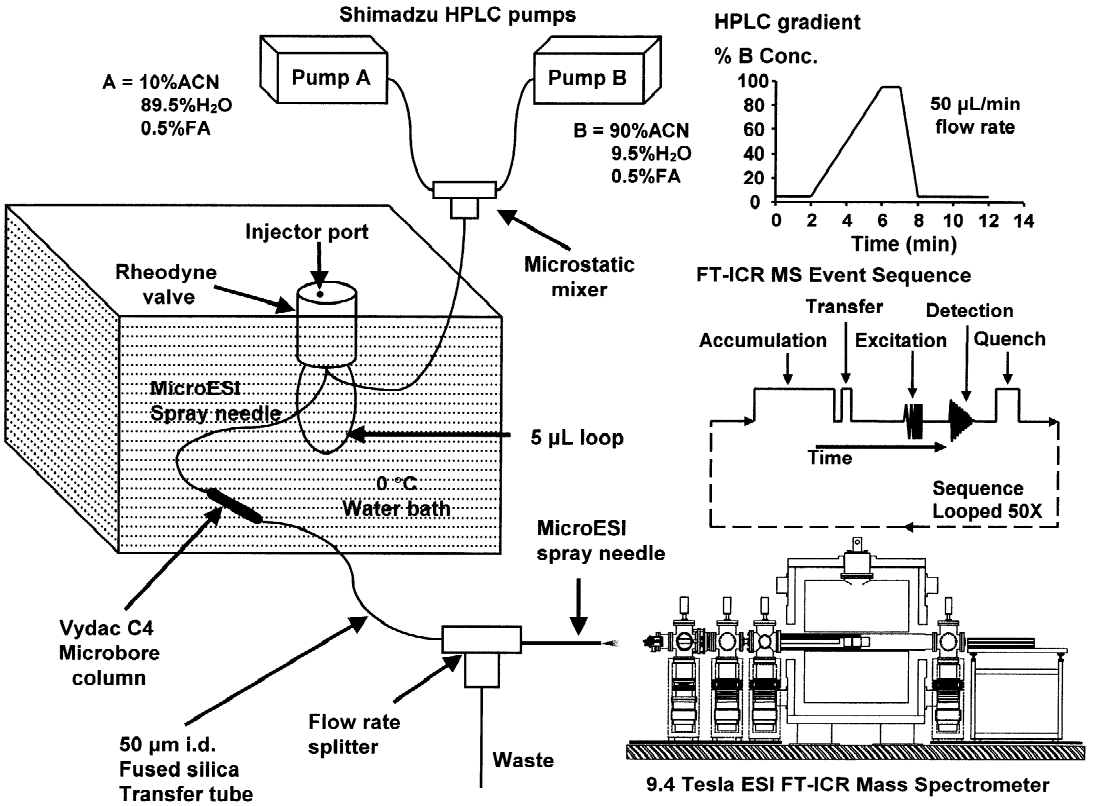

Fig. 1. Configuration for on-line coupling of HPLC–ESI-FT-ICR-MS apparatus. To minimize back exchange (^2H to H), all components from the HPLC injector through the C_4 column are kept on ice. A 4-min gradient (from 10:89.5:0.5, v/v to 90:9.5:0.5, v/v ACN–water–formic acid (FA)) is generated by a pair of Shimadzu HPLC pumps at 50 μl/min. A 50 μm I.D. fused-silica transfer capillary connected to the RP-column to the micro-flow-rate splitter splits 50 μl/min to 350–450 nl/min. A 50 μm I.D. electrospray emitter is directly attached to the splitter. An experimental event sequence (see Section 2) is inserted above the 9.4 T FT-ICR mass spectrometer diagram. Event durations are not exactly to scale.

of protein is needed, and the protein need not be low molecular mass, highly soluble, or crystallizable. The main disadvantages are: (a) care must be taken so that back-exchange of backbone amide hydrogens is minimized (i.e. ^{2}H replaced by H) during the LC–MS process; and (b) the level of spatial detail is limited by the length of the peptic peptides. Fortunately, pepsin has relatively broad proteolytic specificity, so that peptic digestion of even a small protein (M_r~25,000 in this case) can yield dozens of overlapping segments. The *difference* in deuterium uptake between two highly overlapped peptides can then narrow the spatial resolution down to a few (or even one) amide backbone hydrogens. Zhang et al. have shown that H/^{2}H exchange accessibility data from mass spectrometry are consistent with those from NMR, and moreover can span a wider range of H/^{2}H exchange rates [24].

High mass resolution is especially helpful, first in identifying each of the dozens of peptides resulting from peptic digestion of the protein, and second in resolving each of their isotopic envelopes as the various peptides gain mass due to uptake of varying numbers of deuteriums. The peptide isotopic distributions can overlap and even cross over each other during the course of the H/^{2}H exchange experiment. Fourier-transform ion-cyclotron-resonance (FT-ICR) mass spectrometry [25] offers the highest available mass resolving power and mass accuracy [26]. On-line HPLC–microelectrospray (ESI) [27–29] is highly sensitive (10 n*M* or less [30,31]) and serves to desalt and reduce the complexity of the peptic digest.

Here, we apply the H/^{2}H exchange method to map the protein:protein contact interface(s) for in vitro assembled human immunodeficiency virus (HIV-1) capsid protein (CA). At low salt concentration, the CA protein (M_r~25,000) exists in a monomer–dimer equilibrium [32], whereas at high ionic strength it polymerizes into long tube-like structures, consisting of hexamer clustered subunits [33–35]. Those tubes represent a good model for the viral core which itself is an active component of the reverse transcription mechanism [36]. Mutations, which interfere with proper core formation, commonly inhibit viral maturation.

The CA protein is a two-domain protein and high resolution structures of the isolated N- and C-terminal domains are available [32,37,38]. The C-domain crystallized as a dimer whereas the N-terminal domain, solved by NMR, was monomeric. Li et al. investigated the helical assembly of CA hexamer lattice by electron microscopy and image reconstruction [35]. Their reconstruction of the hexamer lattice suggests that the N-terminal domains of the CA protein form hexameric rings, and the C-terminal domains connect the rings. However, the resolution of the image reconstruction was insufficient to arrive at a detailed understanding of the contact regions. Further understanding of the details of assembly of the core proteins could provide a therapeutic target.

2. Experimental

2.1. Protein preparation

Recombinant HIV-1 capsid CA protein was expressed in *Escherichia coli* BL21 (DE3) [39]. Bacterial cells expressing CA proteins were lysed, and capsid proteins were precipitated with ammonium sulfate. Precipitated proteins were resuspended and dialyzed into 25 m*M* Tris–Cl pH 8.1 buffer and purified by Pharmacia High-Trap Q-Sepharose ion-exchange chromatography. Purity was determined by accurate mass by use of ESI-FT-ICR-MS on the monomer subunit (data not shown). The polymerization from monomer to assembled CA (confirmed by scanning electron microscopy, not shown) was initiated by increasing the salt concentration to 1.0 *M* NaCl, and allowing 30 min for assembly at ambient temperature. Hydrogen–deuterium exchange (HDX) was performed on both the monomer CA and assembled CA. Monomer and assembled CA were aliquoted in triplicate for HDX reaction experiments.

2.2. Hydrogen/deuterium exchange experimental procedure

For each hydrogen/deuterium exchange reaction, individual stock solutions of 500 μ*M* purified monomer and hexamer CA protein (in 50 m*M* Na_2HPO_4 at pH 8.0) were prepared and a fresh porcine pepsin (Roche) stock solution of ~80 μ*M* was prepared in 0.5% formic acid (FA). Deuterated buffer (pH 6.8) containing 25 m*M* ammonium acetate (Sigma) in deuterium oxide (Sigma) was prepared fresh. The

assembled CA was diluted into deuterium oxide that also contained 2.0 *M* NaCl, to stabilize the assembled polymers. A stock solution of 0.5% FA, pH 2.1, was used to quench the reaction.

A 2-μl aliquot of stock CA protein solution was mixed with 18 μl of deuterated buffer to initiate $H/^2H$ exchange at room temperature (22.4 °C) for each time period. The CA protein samples were allowed to exchange for periods of 0, 0.5, 1, 2, 4, 8, 16, 30, 60, 120, 240, 480, 960, 2760, and 4080 min. Each exchange time period was run in triplicate. The exchanges were quenched by the addition of 20 μl of quenching solution at the end of the exchange period. Each sample was vortexed, then frozen immediately with liquid nitrogen and stored at −70 °C until on-line LC–MS analysis. The above deuterium exchange procedure was performed separately for soluble and assembled CA. A 4080 min exchange period (i.e. the plateau after which no additional exchange is observed experimentally) served as the ''100%'' control (i.e. maximum achievable exchange of solvent-accessible backbone NH hydrogens). The zero-control (no deuterium exchange) was prepared by adding 20 μl of quenching solution to 2 μl of stock CA protein prior to adding the 18 μl of deuterated buffer. A blank-control (no deuterium exchange) was prepared by adding 20 μl of quenching solution to 2 μl of stock CA protein in buffered H_2O. All controls were also performed in triplicate.

2.3. On-line LC

A Shimadzu HPLC pumping system was used to deliver the solvents. Solutions A and B consisted of 10:89.5 and 90:9.5 acetonitrile–water with 0.5% FA, respectively. A manual injector with a 5-μl loop and an analytical Vydac Microbore column (C_4, 300 Å, 5 μm, 50×1.0 mm) were submerged in a 0 °C ice bath during the experiment. Equal volumes of pepsin in 0.5% FA and CA protein (20 μl pepsin stock solution and 20 μl CA protein sample, 80 μ*M* and 12.5 μ*M*, respectively) were mixed and immediately loaded onto the 0 °C 5-μl loop for CA protein digestion. A 2-min digestion occurred in the loop at 0 °C prior to injection onto the (ice-cold) Vydac C_4 micro-column. A 4-min linear gradient elution profile was used (see Fig. 1). A post column split-flow interface reduced the flow-rate from 50 μl/min from the HPLC system to ~350–450 nl/min for microelectrospray ionization.

2.4. Electrospray ionization FT-ICR mass analysis

A 50-μm inner diameter micro-ESI spray needle [27] was coupled directly to a MicroTee flow-rate splitter (Upchurch), and a 2.0 kV ESI needle voltage was applied to the metal tubing waste line. A heated metal desolvation capillary (3.1 A heating current) was used. The external electrospray interface has been described elsewhere [28]. Mass analyses were carried out with a laboratory-built 9.4 T FT-ICR mass spectrometer configured for external ion accumulation [40]. Fig. 1 shows the FT-ICR-MS experimental event sequence for each exchange sample. Ions were accumulated in a linear octopole ion trap (octopole frequency, 1.5 MHz; amplitude, 240 V_{p-p}) for 2 s and then transmitted to a three-section open cylindrical 4-in.-diameter (1 in.=2.54 cm) Penning trap (trapping voltage, 2 V). Trapped ions were excited (frequency-sweep, 72–320 kHz at 150 Hz/μs, 190 V_{p-p}) and detected (320 kHz Nyquist bandwidth) for 0.8 s to yield 512,000 time-domain data. Typical chamber base pressure was $\sim 5\times10^{-10}$ Torr (1 Torr=133.322 Pa). Time-domain ICR data were acquired by modular FT-ICR-MS data acquisition system (MIDAS) software [41,42]. Fifty time-domain data sets/scans were collected individually during elution of each $H/^2H$ exchange period sample. Peptic fragments of HIV-1 CA appeared only in 7–10 of those data sets. Each experimental time-domain transient data set was baseline corrected, Hanning apodized, and zero filled once prior to fast Fourier transformation (FFT) followed by magnitude calculation. External mass calibration [43,44] was used for the blank-control(s) to assign peptic fragments to within 20 ppm mass accuracy (i.e. ±0.02 Da for an ion of 1000 Da).

3. Results and discussion

3.1. Pepsin digestion

The present goal is to determine the site(s) of contact between CA subunits in the assembled

cylinders, by comparing $H/^2H$ exchange for various peptide segments of the soluble and assembled forms of the protein. $H/^2H$ exchange of the purified protein is carried out in a Tris–Cl buffer at pH 7.4 and at a salt concentration at which the protein maintains its conformational stability, both as a monomer and as assembled CA (no-salt and high salt concentration; 1.0 *M* NaCl, after quenching). Following $H/^2H$ exchange and quenching, the monomeric and assembled samples are pepsin-digested and loaded onto a C_4 column. Pepsin preferentially cleaves on the C-terminal side of F, L, E, W, Y, and I; other residues may also be cleaved at various rates [45]. Porcine pepsin is selected for two reasons: (a) it exhibits optimal activity at pH 2.1 and 0 °C [46,47] (i.e. the conditions for quenching the $H/^2H$ exchange reactions) and (b) its proteolysis is relatively non-specific, thereby generating numerous overlapping fragment peptides to provide a detailed map of $H/^2H$ exchange along the protein backbone. By the same token, that low specificity results in a complex mixture of peptides that must be resolved and identified. Electrospray ionization FT-ICR-MS is especially suited for such analysis, due to its ultra-high mass resolving power and mass accuracy: for example, more than 500 peptides have been resolved in a single FT-ICR mass spectrum of the Glu-C digest of a 191,000 u protein [48].

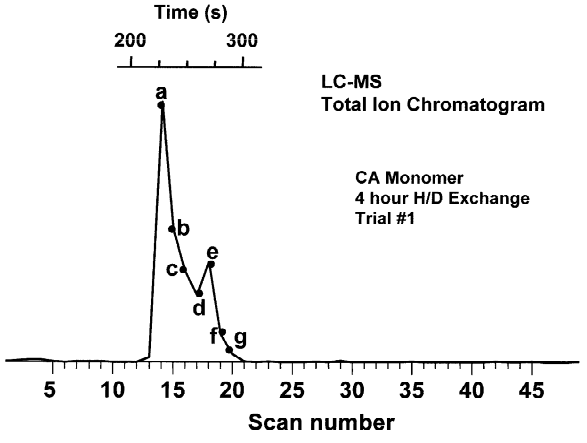

Fig. 2. Representative total ion chromatograph for LC–MS elution of a typical peptide from a C_4 column. Due to the steep gradient required to minimize back exchange, chromatographic separation is not optimal. Nevertheless, high resolution FT-ICR-MS allows for identification of most of the enzymatic peptides from the digest (see Figs. 3 and 4). D, deuterium.

3.2. On-line clean-up

Salt is removed from the sample during a 2-min wash with 5% solution B (~13.5% organic modifier) after the peptic fragments have been loaded onto the column (see HPLC gradient graph in Fig. 1). A 4-min gradient was implemented to maximize separation of the complex peptide mixture while minimizing back-exchange of hydrogen for deuterium. The column was re-equilibrated for 4 min prior to the next $H/^2H$ exchange sample injection. Post-column (rather than pre-column) flow-rate splitting minimizes the time that the peptides reside on the column, further minimizing back-exchange. Post-column splitting reduces the flow-rate to 350–450 nl/min, a rate appropriate for efficient microelectrospray ion generation.

3.3. Data analysis

Fig. 2 shows a total ion chromatogram (TIC) for a typical $H/^2H$ exchange sample. Most of the peptides elute during a period of ~1.5 min. The TIC resolution depends on the scan rate, which depends on the data acquisition period. Note that an average scan contains more than 20 different peptides (see Fig. 3). Although the LC reduces somewhat the complexity of the mixture, the principal separation is provided by mass resolution. A given peptide elutes in two to four mass spectral scans because of the steep gradient of the eluent (see the stars in scans a, b, c, and d of Fig. 3).

The blank-control (no $H/^2H$ exchange) serves to determine the CA protein sequence coverage. THRASH, a program developed by Horn et al., was used to identify the peptic fragments and assign accurate isotopic mass [49]. Peptides containing 95% of the amino acids of the CA protein sequence (see Fig. 4) were found in the blank-control mass spectra. The identified peptic fragments form the basis for mass centroid determination, and thus the number of exchanged hydrogens. Fig. 6 also reveals a large number of peptides with overlapping primary sequences. A difference in $H/^2H$ exchange extent between two highly overlapped peptides can focus

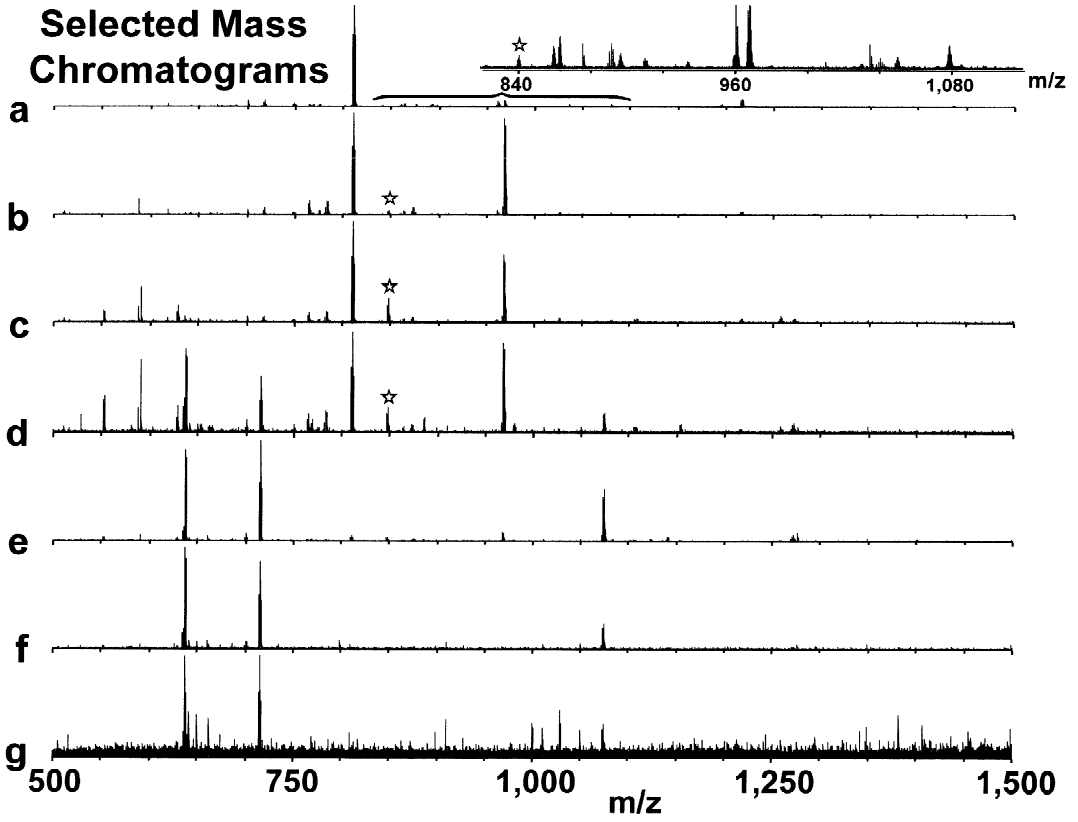

Fig. 3. Mass spectra at various stages of LC elution. Mass spectra (a)–(g) correspond to scans (a)–(g) in Fig. 2. The inset above spectrum (a) (top right) illustrates the spectral complexity. The minimum threshold for identification of peptic fragments was a peak signal-to-noise ratio of 3. No peptic fragments were observed beyond m/z 1500.

the H/^{2}H exchange down to a few backbone amide hydrogens (sometimes, even one) [24]. For example, in the primary sequence segment extending from the bottom of helix I to the beginning of helix II (fragment 23–40), Fig. 4 shows that there are several overlapping peptic peptides. Comparison of the exchange rates for each of those peptides reveals that the exchange rate is higher in the loop connecting helices I and II than in either of the adjoining alpha helices. The high mass resolving power of FT-ICR-MS permits the identification of peptide mass doublets differing by less than 40×10^{-3} u (see Fig. 5).

Fig. 5 shows the mass spectral resolving power required to distinguish the isotopic distributions of two H/^{2}H exchanged peptides of similar mass. The two peptides shift to higher mass with deuterium incorporation (see 30 s spectral inset of Fig. 5) and increase the complexity of peak assignments for mass centroid determination. The following equation was implemented in MIDAS analysis to calculate each peptic fragment's mass centroid (M_c):

$$M_c = \frac{\sum(m_i I_i)}{\sum I_i} \quad (1)$$

in which m_i and I_i are the isotopic peak mass and relative abundance, respectively, of a given peptic fragment's isotopic mass distribution. Each calculated mass centroid is then plotted as a function of exchange period, and the curve is obtained by a third degree polynomial fit (see Fig. 6).

3.4. Deuterium back-exchange

The back-exchange (^{2}H to H exchange) ultimately determines the uncertainty of structural information

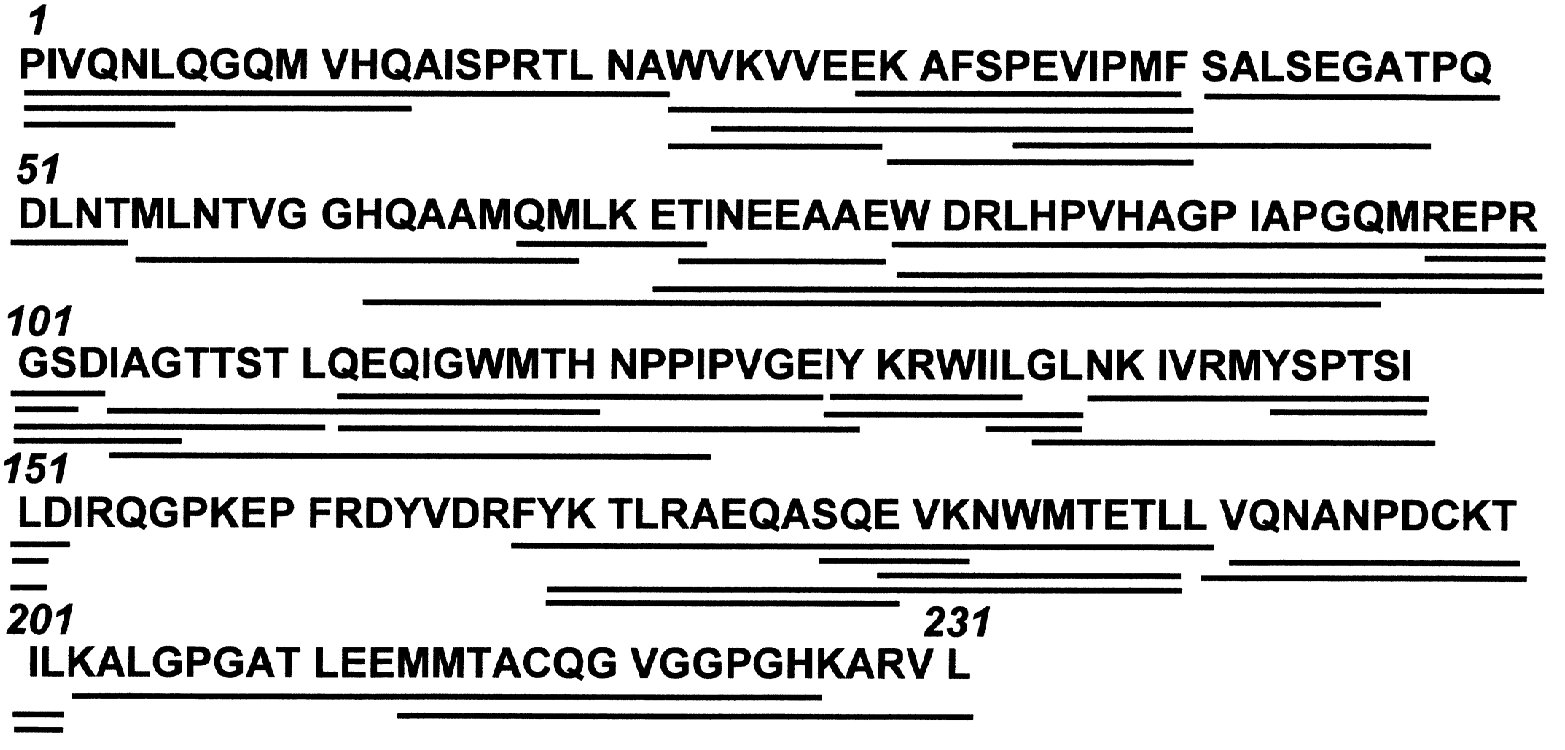

Fig. 4. Amino acid sequences of observed peptic fragments of HIV-1 capsid CA protein, spanning 95% of the protein primary sequence (215 of 231 amino acids). Overlapping coverage greatly enhances the specificity of the mapping of the contact surfaces in the protein hexamer.

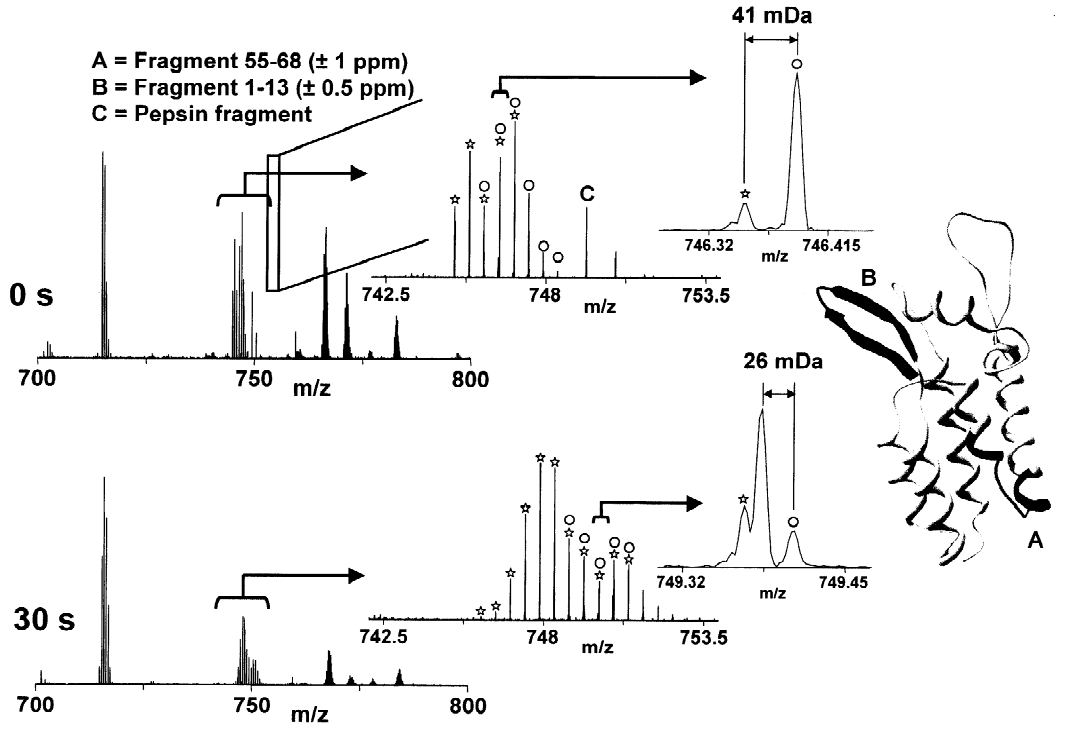

Fig. 5. High-resolution spectra of two peptides (A and B, shaded in black at right) of similar masses. The inset shows the separation capability of FT-ICR-MS for proper peak assignments for centroid mass determination. The two central insets show the shifts of isotopic peak distributions of peptides A and B to high mass after 30 s H/^{2}H exchange period. The upper insets show that peaks with mass differences greater than 26×10^{-3} u are baseline resolved.

from a H/^{2}H exchange experiment. The deuterium content ($^2H_{H\rightarrow{}^2H}$) for each peptide may be calculated from the following [21]:

$$^2H_{H\rightarrow{}^2H} = \frac{m - m_{0\%}}{m_{100\%} - m_{0\%}} N \quad (2)$$

in which N is the total number of exchangeable hydrogens calculated from Eq. (3). In Eq. (2), $m_{0\%}$, m, and $m_{100\%}$ are isotopic averaged centroids of the molecular ion peaks for the zero-control, assigned peptide, and 100%-control, respectively:

$$N = (A) - (P) - 1 \quad (3)$$

In Eq. (3), A and P are the number of amino acids and proline residues in the peptide; and the number ''1'' accounts for the N-terminus hydrogen that back exchanges rapidly. Note that the various exchangeable side-chain hydrogens are not included in Eq. (3) because their back-exchange rates are much faster than those of amide hydrogens [24]. Essentially complete back-exchange of side-chain deuteriums likely occurs during three stages prior to ESI-FT-ICR-MS: sample thawing, the 2-min peptic digestion in the loop, or loading/washing/elution LC. The % back exchange ($\%^2H_{^2H\rightarrow H}$) may then be calculated as:

$$\%^2H_{^2H\rightarrow H} = \frac{N - (m_{100\%} - m_{0\%})}{N} \cdot 100\% \quad (4)$$

The 100%-control (4080 min exchange period) shows a back-exchange (backbone NH hydrogens only) of about 20% for the CA protein fragment 1–22 (2414.285 u neutral mass). Most of the NH back-exchange occurs during thawing and the 2-min desalting period (100 μl solvent, ~2× solvent-accessible column volume). The 2-min digestion in the 5-μl loop should have a minimal effect on back-exchange because it is carried out at 0 °C and at pH

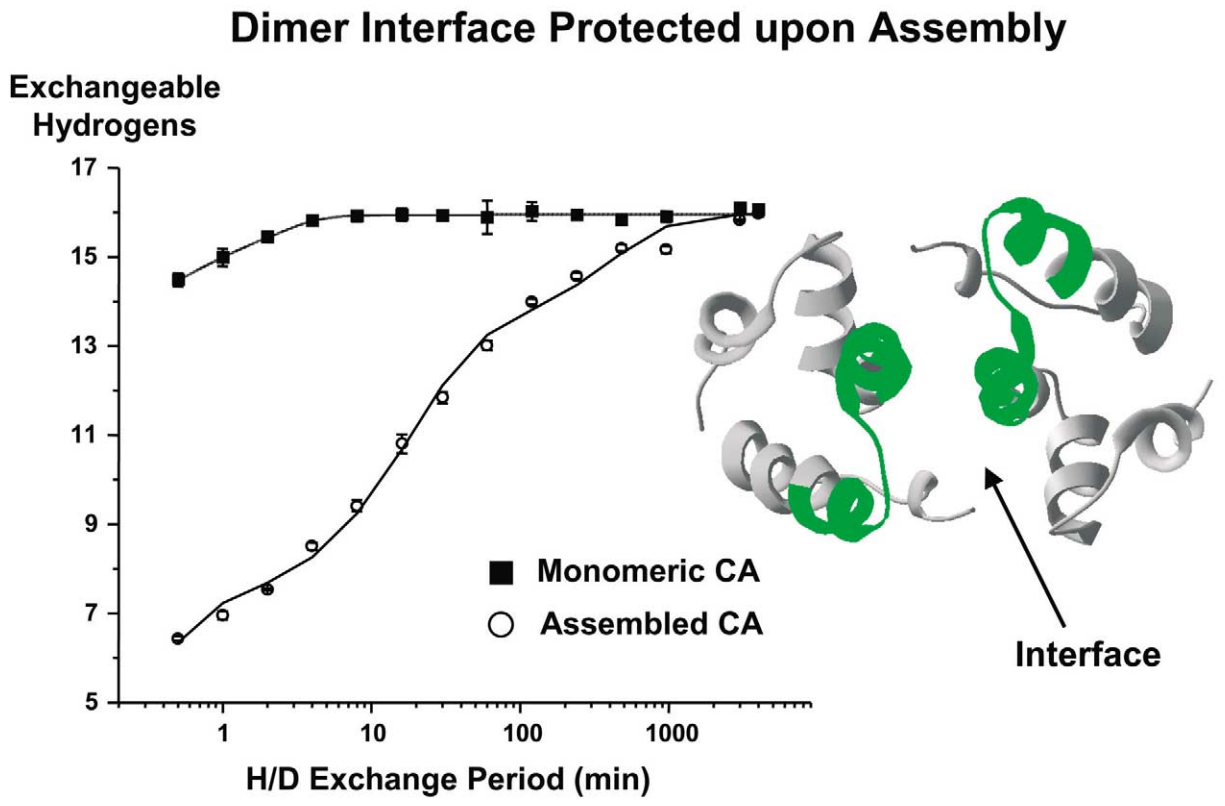

Fig. 6. H/^{2}H exchange vs. time profiles for a peptide segment (dimer interface, shown in green at right, located at the C-terminus domain) in monomeric (■) and hexameric (○) CA protein. The much slower H/^{2}H exchange for the hexamer relative to the monomer shows that helix IX is highly protected against exchange in the assembled CA, presumably because that segment is located at the protein:protein contact surface in the complex.

2.3. (Desalting was also carried out at 0 °C and pH 2.1. However, desalting occurs during solvent flow (~100 μl solvent total volume), whereas digestion occurs in a non-flowing solvent system (~5 μl solvent total volume). Therefore back-exchange should be much less during digestion than desalting.) We calculated the % back exchange for other fragments as well. Fragment 1–22 was chosen for presentation because that peptide is known to be completely solvent accessible in the protein's stable conformation, and hence is ideal for calculating back-exchange. The average back-exchange was estimated as 20–30% for all of the assigned peptic peptides.

Deuterated peptide NH back-exchange could occur in the gas phase by collisions with water molecules in the vacuum chamber. We minimized adsorbed water by heating the accumulation octopole (i.e. the highest pressure chamber in the FT-ICR instrument, $\sim 4\times10^{-6}$ Torr), where back-exchange would be most likely to occur. Once the ions are trapped in the ICR cell, the pressure is so low ($\sim 5\times10^{-10}$ Torr) that back-exchange of the deuterated ions should be negligible.

3.5. Mapping the protein:protein binding surface

Fig. 6 shows how the mass centroid for peptide fragment 169–189 increases as a function of the logarithm of the H/^{2}H exchange period (the logarithmic scale compresses the graph so that the changes can be visualized over a long exchange period). (Note that it is the exchange *rate* that is important, because all of the backbone amide hydrogens will

exchange eventually.) Note that the peptide fragment 169–189 is more protected against H/^{2}H exchange in the assembled hexamer than in the monomer, and thus presumably participates in the protein:protein interactions that form the hexamer tube. Moreover, peptide fragment 169–189 includes the nine backbone amide hydrogens known to reside at the CA dimer interface (green in Fig. 6) thus, the dimer interface observed in the crystal structure of the isolated domain [35] is evidently also important in the formation of the tube composed of the intact protein. H/^{2}H exchange for numerous other fragments of monomeric and assembled CA have been analyzed and will be discussed in detail elsewhere.

4. Conclusion

Hydrogen/deuterium exchange, monitored by high resolution FT-ICR-MS provides a rapid (1 day data collection) and efficient means for mapping protein:protein interaction surface(s). The experimental design described in Section 2 and Fig. 1 is highly reproducible and demonstrates that high-mass protein complexes can be analyzed by this method.

On-line LC front-end separation prior to micro-ESI-FT-ICR aids in reduction of the overall complexity of the sample, desalts the sample eliminating salt adducts with the peptides, and minimizes the ^{2}H/H back exchange. We are currently working to reduce ^{2}H/H back exchange even more, so as to determine exchange rates more accurately for smaller peptic fragments.

Acknowledgements

We acknowledge John Quinn's technical assistance and give special thanks to David Horn and Greg Blakney for providing THRASH and modification to MIDAS analysis to facilitate monoisotopic peak determination and centroid determination. Work supported by NSF (CHE-99-09502), NIH (GM-31683; AI-44626), Florida State University, and the National High Magnetic Field Laboratory in Tallahassee, FL.

References

[1] B. Kojic-Prodic, J. Kroon, Croatica Chem. Acta 74 (2001) 1.
[2] G. Scapin, A.C.M. Young, A. Kromminga, J.H. Veerkamp, J.I. Gordon, J.C. Sacchettini, Mol. Cell. Biochem. 123 (1993) 3.
[3] A.E. Sauereriksson, G.J. Kleywegt, M. Uhl, T.A. Jones, Structure 3 (1995) 265.
[4] K.E. McAuley, P.K. Fyfe, J.P. Ridge, N.W. Isaacs, R.J. Cogdell, M.R. Jones, Proc. Natl. Acad. Sci. USA 96 (1999) 14706.
[5] A.G. Palmer, Annu. Rev. Biophys. Biomol. Struct. 30 (2001) 129.
[6] G. Wider, Biotechniques 29 (2000) 1278.
[7] J.X. Song, F. Ni, Biochem. Cell Biol.–Biochim. Biol. Cell. 76 (1998) 177.
[8] L.E. Kay, Biochem. Cell Biol.–Biochim. Biol. Cell. 75 (1997) 1.
[9] A.G. Palmer, J. Williams, A. McDermott, J. Phys. Chem. 100 (1996) 13293.
[10] S.W. Englander, M.M.G. Krishna, Nat. Struct. Biol. 8 (2001) 741.
[11] S.W. Englander, A.J. Wand, Biochemistry 26 (1987) 5953.
[12] S.W. Englander, N.R. Kallenbach, Q. Rev. Biophys. 16 (1984) 18.
[13] C. Woodward, I. Simon, E. Tuchsen, Mol. Cell. Biochem. 48 (1982) 135.
[14] A. Demarco, M. Llinas, K. Wuthrich, Biopolymers 17 (1978) 637.
[15] I.D. Campbell, C.M. Dobson, G. Jeminet, R.J. Williams, FEBS Lett. 49 (1974) 115.
[16] M. Tashiro, R. Tejero, D.E. Zimmerman, B. Celda, B. Nilsson, G.T. Montelione, J. Mol. Biol. 272 (1997) 573.
[17] H. Takahashi, T. Nakanishi, K. Kami, Y. Arata, I. Shimada, Nat. Struct. Biol. 7 (2000) 220.
[18] T. Sivaraman, T. Krishnaswamy, S. Kumar, C. Yu, Biochemistry 38 (1999) 9899.
[19] C.J. Craven, N.M. Derix, J. Hendriks, R. Boelens, K.J. Hellingwerf, R. Kaptein, Biochemistry 39 (2000) 14392.
[20] K.H. Gardner, L.E. Kay, Annu. Rev. Biophys. Biomol. Struct. 27 (1998) 357.
[21] Z. Zhang, D.L. Smith, Protein Sci. 2 (1993) 522.
[22] D.L. Smith, Y. Deng, Z. Zhang, J. Mass Spectrom. 32 (1997) 135.
[23] A. Miranker, C.V. Robinson, S.E. Radford, R.T. Aplin, C.M. Dobson, Science 262 (1993) 896.
[24] Z.Q. Zhang, W.Q. Li, T.M. Logan, M. Li, A.G. Marshall, Protein Sci. 6 (1997) 2203.
[25] A.G. Marshall, C.L. Hendrickson, G.S. Jackson, Mass Spectrom. Rev. 17 (1998) 1.
[26] A.G. Marshall, Int. J. Mass Spectrom. 200 (2000) 331.
[27] M.R. Emmett, R.M. Caprioli, J. Am. Soc. Mass Spectrom. 5 (1994) 605.
[28] M.W. Senko, C.L. Hendrickson, L. PasaTolic, J.A. Marto, F.M. White, S.H. Guan, A.G. Marshall, Rapid Commun. Mass Spectrom. 10 (1996) 1824.

[29] M.R. Emmett, F.M. White, C.L. Hendrickson, S.D.-H. Shi, A.G. Marshall, J. Am. Soc. Mass Spectrom. 9 (1998) 333.
[30] T.L. Quenzer, M.R. Emmett, C.L. Hendrickson, P.H. Kelly, A.G. Marshall, Anal. Chem. 73 (2001) 1721.
[31] P.E. Andren, M.R. Emmett, R.M. Caprioli, J. Am. Soc. Mass Spectrom. 5 (1994) 867.
[32] T.R. Gamble, S.H. Yoo, F.F. Vajdos, U.K. von Schwedler, D.K. Worthylake, H. Wang, J.P. McCutcheon, W.I. Sundquist, C.P. Hill, Science 278 (1997) 849.
[33] L.S. Ehrlich, B.E. Agresta, C.A. Carter, J. Virol. 66 (1992) 4874.
[34] S. Campbell, V.M. Vogt, J. Virol. 69 (1995) 6487.
[35] S. Li, C.P. Hill, W.I. Sundquist, J.T. Finch, Nature 407 (2000) 409.
[36] S.X. Tang, T. Murakami, B.E. Agresta, S. Campbell, E.O. Freed, J.G. Levin, J. Virol. 75 (2001) 9357.
[37] R.K. Gitti, B.M. Lee, J. Walker, M.F. Summers, S. Yoo, W.I. Sundquist, Science 273 (1996) 231.
[38] G. Momany, L.C. Kovari, A.J. Prongay, W. Keller, R.K. Gitti, B.M. Lee, A.E. Gorbalenya, L. Tong, J. McClure, L.S. Ehrlich, M.F. Summers, C. Carter, M.G. Rossmann, Nat. Struct. Biol. 3 (1996) 763.
[39] J.K. Lanman, J. Sexton, M. Sakalian, P.E. Prevelige, Jr., J. Virol. 76 (2002) 6900.
[40] M.W. Senko, C.L. Hendrickson, M.R. Emmett, S.D.H. Shi, A.G. Marshall, J. Am. Soc. Mass Spectrom. 8 (1997) 970.
[41] M.W. Senko, J.D. Canterbury, S.H. Guan, A.G. Marshall, Rapid Commun. Mass Spectrom. 10 (1996) 1839.
[42] G.T. Blakney, G. van der Rest, J.R. Johnson, M.A. Freitas, J.J. Drader, S.D.-H. Shi, C.L. Hendrickson, N.L. Kelleher, A.G. Marshall, in: Proceedings of the 49th American Society of Mass Spectrometry Conference on Mass Spectrometry and Allied Topics, American Society of Mass Spectrometry, Chicago, IL, 2001, p. WPM265.
[43] E.B. Ledford Jr., D.L. Rempel, M.L. Gross, Anal. Chem. 56 (1984) 2744.
[44] S.D.-H. Shi, J.J. Drader, M.A. Freitas, C.L. Hendrickson, A.G. Marshall, Int. J. Mass Spectrom. 195–196 (2000) 591.
[45] G. Sachdev, J. Fruton, Biochemistry 9 (1970) 4465.
[46] A. Cornish-Bowden, J. Knowles, Biochem. J. 113 (1969) 353.
[47] W. Konigsberg, J. Goldstein, R.J. Hill, J. Biol. Chem. 238 (1963) 2028.
[48] F.W. McLafferty, E.K. Fridriksson, D.M. Horn, M.A. Lewis, R.A. Zubarev, Science 284 (1999) 1289.
[49] D.M. Horn, R.A. Zubarev, F.W. McLafferty, J. Am. Soc. Mass Spectrom. 11 (2000) 320.